INVESTIGATION OF THE CONSTANT CURVATURE KINEMATIC ASSUMPTION OF A 2-DOFS CABLE-DRIVEN CONTINUUM ROBOT

Ammar AMOURI[1]

Despite many research attempts, continuum robots modeling has been proven to be complex and challenging. Most of the proposed kinematic contributions and approaches mentioned in literature were only established on the basis of constant curvature kinematic assumption (CCKA). For this reason, the current study aims to investigate the validity of the CCKA for a class of continuum robots called Cable-Driven Continuum Robot (CDCR) using Matlab and nonlinear dynamic Solidworks software as well as experimental measurements. The CAD model of CDCR was firstly introduced; then, the forward kinematic model was established. Simulations using both software on the CDCR were carried out so that a comparison can take place between the obtained results from simulations and the experimental measurements.

Keywords: Continuum robot, cable-driven continuum robot, kinematic modeling, constant curvature kinematic assumption, nonlinear dynamic solidworks simulation.

1. Introduction

In the past two decades, continuum robots design and modeling have attracted much interest from robotics researchers for many advantages, such as high dexterity, low inertia and having an unconventional structure. The morphology and operation of these robots are similar to elephant trunks, snakes, tentacles.

Currently, a number of hard and soft continuum robots have been presented in [1-2]. The conceptual design of the hard class namely cable-driven continuum robot came up firstly in 2000 through research made by a research group of Clemson University [3]. It is such a hyper-redundant robot built on the basis of the following elements: a flexible backbone, rigid spacer disks, cables and a rigid base which includes the control system. Generally, one bending section of CDCR has two rotational DOFs with respect to its fixed base.

The complexity of computing the kinematic models of continuum robots makes researchers use some approximations and hypotheses. The common hypothesis for continuum robots modeling is the constant curvature kinematic

[1] Department of Mechanical Engineering, University of Brothers Mentouri, Constantine 1, Algeria, e-mail: ammar_amouri@yahoo.fr

assumption (CCKA). This approximation has the advantage to simplify the kinematic models formulation [4]. However, most kinematic contributions have been developed on the basis of CCKA such as [4-15], employing different methods and theories, such as arc geometry, Frenet-Serret frames, Euler-Bernoulli beam equation and Denavit-Hartenburg parameters.

According to the literature review, the constant curvature kinematic assumption is employed for continuum robot in the absence of external loading and a uniform distribution of the internal loading [1, 3, 7]. To our best knowledge, no explicit study has been presented validating this hypothesis; therefore, this paper aims, at first, designing and developing the FKM of 2-DOFs CDCR under constant curvature kinematic assumption; then, the investigation of this hypothesis is performed by using Matlab and nonlinear dynamic Solidworks software. Besides, experimental measurements using 3D portable measuring arm have been carried out.

The paper is organized as follows: in Section 2 the CAD model design and the description of CDCR are presented. In Section 3, the forward kinematic model is derived under the constant curvature kinematic assumption. In Section 4, Matlab and nonlinear dynamic Solidworks software are used to examine the constant curvature kinematic assumption through simulations followed by verification using experimental measurements. Afterwards, a comparison of results is made. Finally, Section 5 concludes the paper.

2- Description of the CDCR and kinematic nomenclature

Fig. 1 shows the CAD model of the designed CDCR which is composed of one bending section. The principal components of this robot are: a flexible backbone, three inextensible cables, and a number of spacer disks with three pinholes on each one used to guide the cables. The arrangement of pinholes on the disk is shown in the right side of Figure 2. The spatial motion (i.e. 2-DOFs: 1-DOF for the bending motion and 1-DOF for the orientation motion, see Figure 2) can be governed by deflection of the flexible backbone by applying adequate electrical voltages to one or two motors simultaneously in order to generate tensions on the cables.

In order to describe the CDCR in accordance with the structural design presented in Figure 1, two reference frames are defined: the first one is attached to the fixed disk $\Re_0\left(X_0, Y_0, Z_0\right)$ and the second frame is situated at the end of the disk $\Re\left(X, Y, Z\right)$. The central axis of the CDCR is modeled by an inextensible arc of circle, oriented in space and parameterized by its arc length ℓ, a curvature κ, and an orientation angle φ. The bending angle θ is measured in the bending plane which is always perpendicular to the X_0Y_0 plane and rotates around Z_0-axis

(Fig. 2). The following symbols, variables and parameters are used in the following sections:

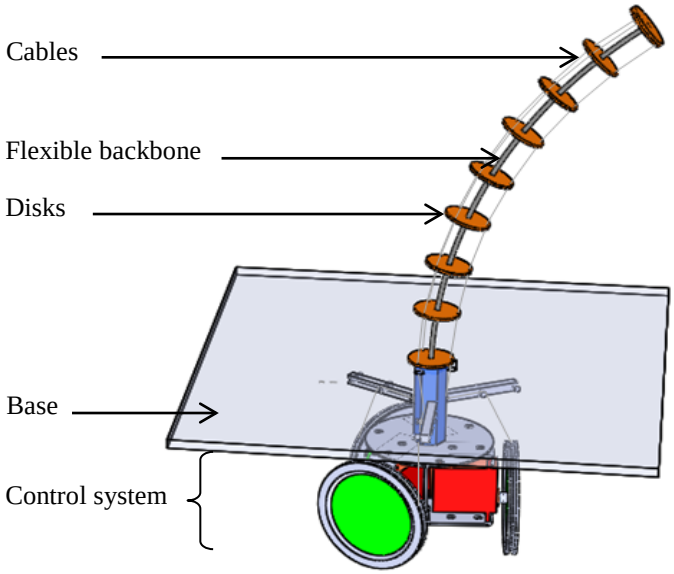

Fig. 1. CAD model of the CDCR

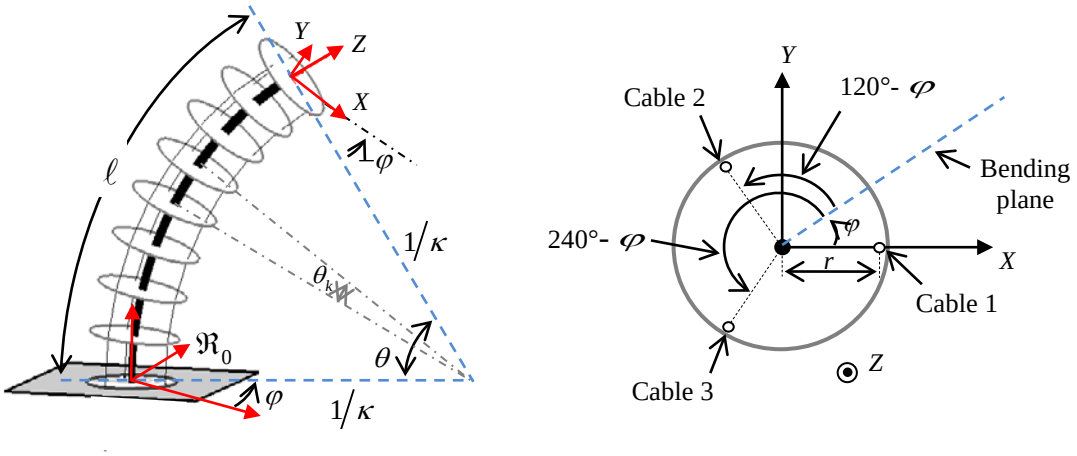

Fig. 2. Description of the CDCR and its kinematic nomenclature

- i is the index of cable, $i = 1, 2, 3$;
- ℓ is the length of flexible backbone;
- ℓ_i is the length of cable i;
- n is the number of modules composing the CDCR, $n = 1, 2, 3, ..., N$;
- k is the index of considered module;

- r is the radial distance between the cables and the central axis of flexible backbone;
- (X, Y, Z) is the Cartesian coordinates of the flexible backbone's tip;
- $(\theta, \varphi, \kappa)$ is the arc parameters: the bending angle θ, the orientation angle φ and the curvature κ.

3. Constant Curvature Kinematic Modeling

This section details the methodology of deducing the forward kinematic model (FKM) of the CDCR under consideration. In the following development, three spaces are used to describe the CDCR states. The global view of the kinematic modeling is shown in Fig. 3.

Thus, on the basis of constant curvature kinematic assumption and assuming that the flexible backbone has a high stiffness to avoid possible twisting motions about its axial axis, the operational coordinates X can be expressed as a function of arc parameters K as follows (see Fig. 2):

$$\begin{cases} X = \dfrac{2}{\kappa}\sin^2\left(\dfrac{\theta}{2}\right)\cos(\varphi) \\ Y = \dfrac{2}{\kappa}\sin^2\left(\dfrac{\theta}{2}\right)\sin(\varphi) \\ Z = \dfrac{1}{\kappa}\sin(\theta) \end{cases} \tag{1}$$

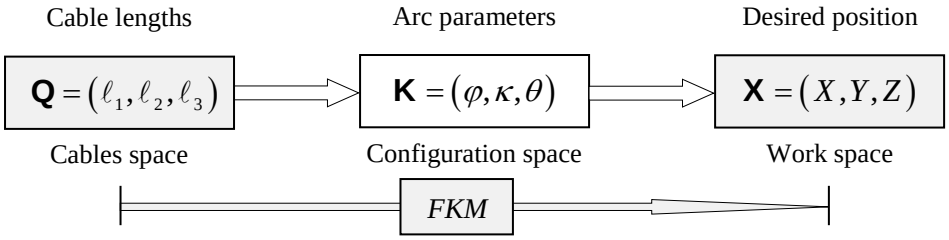

Fig. 3. Global view of the CDCR modeling

On the other hand, to express the arc parameters $(\theta, \varphi, \kappa)$ as a function of cable lengths Q, the structure of the CDCR is assimilated to a serial concatenation of n identical modules (see Figure 4).

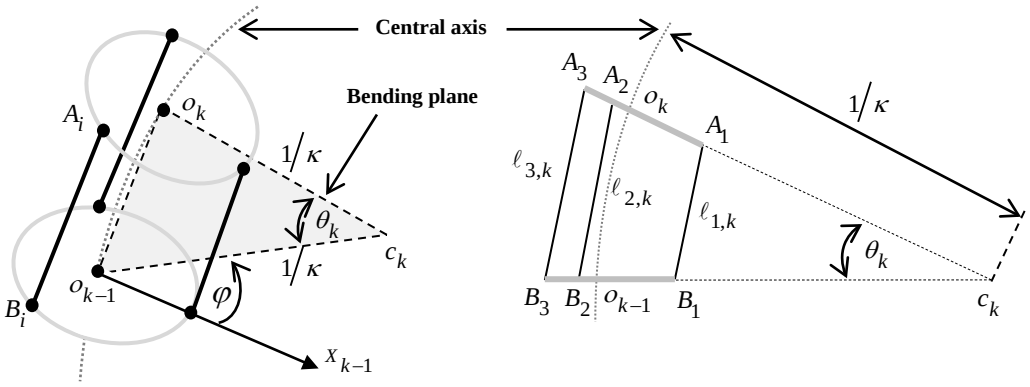

a. 3D representation b. Projection in the bending plane

Fig. 4. Geometry of single module

Because the structure of CDCR is divided to n identical modules (i.e. $\ell_i = n.\ell_{i,k}$), the arc parameters $(\varphi, \kappa, \theta)$ can be written as:

$$\varphi = \tan^{-1}\left(\frac{\sqrt{3}(\ell_3 - \ell_2)}{\ell_2 + \ell_3 - 2\ell_1}\right) \tag{2}$$

$$\kappa = \frac{2\sqrt{\ell_1^2 + \ell_2^2 + \ell_3^2 - \ell_1\ell_2 - \ell_1\ell_3 - \ell_2\ell_3}}{r\,(\ell_1 + \ell_2 + \ell_3)} \tag{3}$$

$$\theta = \frac{2\sqrt{\ell_1^2 + \ell_2^2 + \ell_3^2 - \ell_1\ell_2 - \ell_1\ell_3 - \ell_2\ell_3}}{3r} \tag{4}$$

Finally, the operational coordinates can be expressed as:

$$\begin{cases} X = \dfrac{rL_{sum}}{L_{sqrt}}\sin^2\left(\dfrac{L_{sqrt}}{3r}\right)\cos\left(\tan^{-1}\left(\dfrac{\sqrt{3}(\ell_3 - \ell_2)}{\ell_2 + \ell_3 - 2\ell_1}\right)\right) \\ Y = \dfrac{rL_{sum}}{L_{sqrt}}\sin^2\left(\dfrac{L_{sqrt}}{3r}\right)\sin\left(\tan^{-1}\left(\dfrac{\sqrt{3}(\ell_3 - \ell_2)}{\ell_2 + \ell_3 - 2\ell_1}\right)\right) \\ Z = \dfrac{rL_{sum}}{L_{sqrt}}\sin\left(\dfrac{2L_{sqrt}}{3r}\right) \end{cases} \tag{5}$$

where: $L_{sum} = \ell_1 + \ell_2 + \ell_3$, and $L_{sqrt} = \sqrt{\ell_1^2 + \ell_2^2 + \ell_3^2 - \ell_1\ell_2 - \ell_1\ell_3 - \ell_2\ell_3}$.

4. Simulation and experimental test

Nowadays, simulation is one of the most important techniques for evaluating the research results [16-18]. Therefore, in order to investigate the validity of constant curvature kinematic assumption for the class of continuum robots under consideration, Matlab and Solidworks software were used to examine this hypothesis. At first, the virtual CDCR was simulated, by using nonlinear dynamic Solidworks simulation. At the same time, the Cartesian coordinates of the flexible backbone's tip have been determined and saved. Secondly, for the given values of the cable lengths, used as inputs to FKM, the Cartesian coordinates (outputs) were determined by using Matlab software. Finally, the obtained simulation results were compared to experimental measurements.

4.1. Nonlinear dynamic Solidworks simulation

In quasi-static mode, it is classically accepted under the linear hypothesis that the variation of the cable elongation is proportional to the applied force; therefore, the Solidworks simulation can be performed.

In dynamical analysis, Solidworks simulation may use one of two methods: linear modal simulation and nonlinear dynamic simulation. The second method can be used to compute different physical quantities, such as the displacement field, stresses and strains, at each time step, taking into accounts the applied loads. In this study, the second method was used; thus, for the applied force on the cable 1 of 0 to 80 N, the simulation outputs (i.e. Cartesian coordinates of the flexible backbone's tip) are illustrated in Fig. 5. The discussion of the obtained results is given in subsection 4.4. The estimated parameters of the CDCR are given in Table 1.

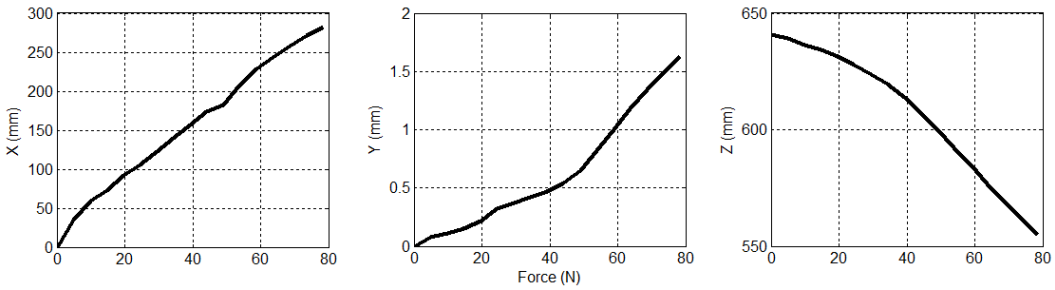

Fig. 5. Solidworks simulation outputs

Table 1

CDCR Parameters

Parameter	Designation	Value
ℓ	Flexible backbone length	641 mm
d	Flexible backbone diameter	5 mm
r	Radial distance between the cables and the central axis	29 mm
E	Young's modulus	35 MPa

4.2. Matlab simulation

The FKM expressed in Equation 5 has been imported to Matlab software in order to plot the outputs of the flexible backbone's tip (i.e. the Cartesian coordinates (X, Y, Z)) as a function of a given cable lengths variation.

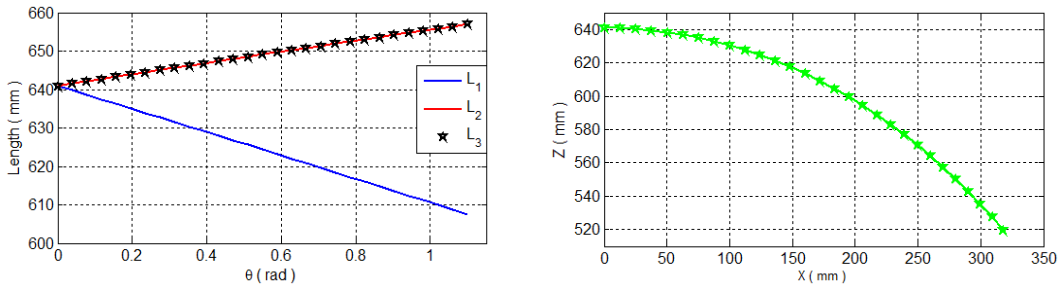

a. The variation of lengths in three cables. b. Cartesian coordinates of the flexible backbone's tip

Fig. 6. Inputs and outputs of the FKM simulation by using Matlab software

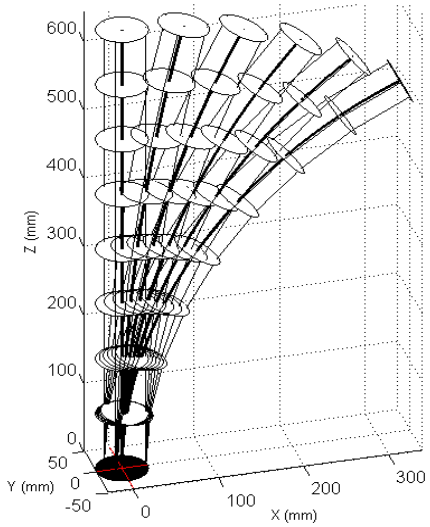

Fig. 7. Some configurations of the CDCR behavior for the given values of the cable lengths

This study has been performed by varying ℓ_i, for $i = 1, 2, 3$, with a given quantity $\Delta\ell$, such as: $\ell_1 = \ell - \Delta\ell$ and $\ell_2 = \ell_3 = \ell + \Delta\ell/2$. Fig. 6 shows the Cartesian coordinates of the flexible backbone's tip relative to the given values of the variation of cable lengths. Some configurations of the CDCR behavior are shown in Fig. 7. The analysis and discussion of the obtained results are provided in subsection 4.4.

4.3. Experimental test procedure

The purpose of these basic experiments is to estimate the evolution of the Cartesian coordinates of the flexible backbone's tip by applying a tension forces on cable 1 (i.e. by means of hanging known weights). The test bench is shown in Figure 8 and is composed of the following [19]:

- The CDCR prototype composed of one bending section. The main component of CDCR is the flexible backbone, along which are rigidly mounted nine spacer disks to guide three inextensible cables by the pinholes in it. The flexible backbone is made of composite materials which makes the robot flexible and lightweight;
- 3D portable measuring arm (FARO Edge/FARO Laser Scan Arm, Model 14000). Its role is to measure the Cartesian coordinates of the flexible backbone's tip with respect to its reference frame (i.e. as an external Cartesian position sensor). The measurement accuracy of 3D measuring arm is ±0.020 mm;
- A set of different masses used as a loading weight to apply a tension force on the cable 1.

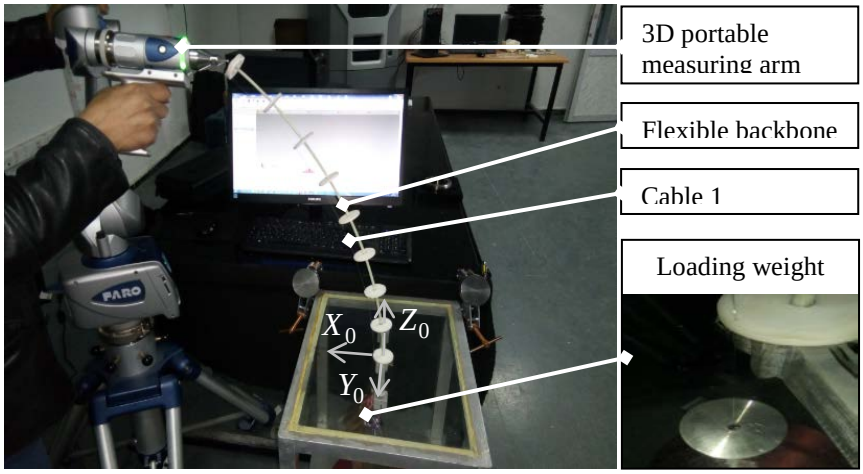

Fig. 8. Overview of the test bench measurement

To perform experimental measurements, the reference frame of 3D portable measuring arm has been transformed to the frame $\Re_0\left(X_0, Y_0, Z_0\right)$ attached to fixed base of CDCR (see Fig. 8). This technique allows to measure the Cartesian coordinates of the flexible backbone's tip with respect to its reference frame without going through the use of homogeneous transformation matrices. Then, for each experiment (i.e. for each hanging weight on the cable 1), the Cartesian coordinates of flexible backbone's tip has been measured and saved using 3D portable measuring arm. The measured Cartesian coordinates for attached weights of $0:0.5:8\ (Kg)$ on the cable 1 are presented in Fig. 9. The analysis and discussion of the obtained results are provided in the following subsection. However, it should be mentioned that there are some sources of measurement uncertainty such as: the initial positioning of the CDCR and the 3D portable measuring arm, and the manual placement of the pointer (FARO probe) on the marker point during each data measure.

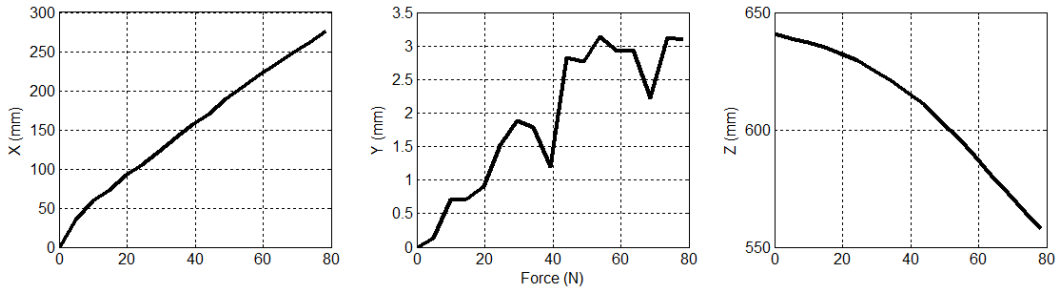

Fig. 9. Measured Cartesian coordinates of the flexible backbone's tip

4.4. Results and discussion

Fig. 10 shows the Cartesian coordinates of the flexible backbone's tip issued from forward kinematic model, by using Matlab software, and those obtained by Solidworks simulation and experimental measurements. The curves show that there is a considerable convergence between them. The associated Euclidean errors along each axis, relative to applied force, are shown in Figures 11 and 12, where the mean error is smaller than 4.95 mm between CCKA and Solidworks simulation and 2.4 mm between CCKA and experimental measurements. Those errors represent, respectively, 0.77 % and 0.37 % of the robot length. On the other hand, it is important to notice that the measurement errors may be caused by: (i) the gravity effects of CDCR components when taking measurements while they were ignored in simulation operation, (ii) existence of friction forces between cables and disks, (iii) the stiffness bending of the flexible backbone constituted of composite materials which is not well estimated.

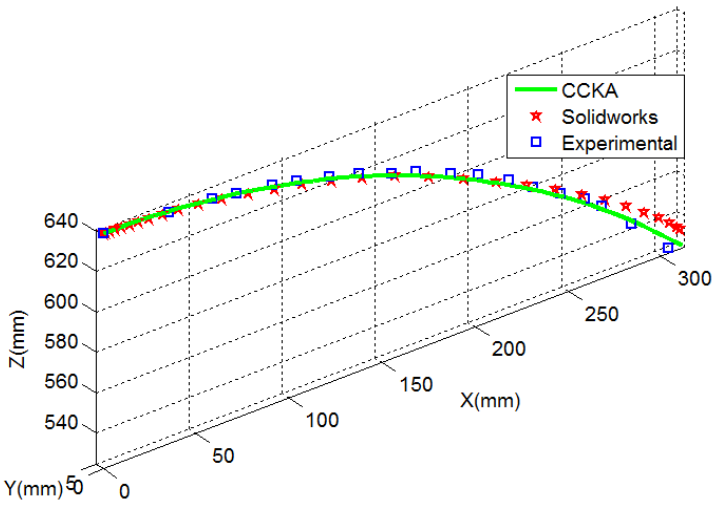

Fig. 10. Cartesian coordinates of the flexible backbone's tip obtained by Matlab and Solidworks software, and experimental measurements

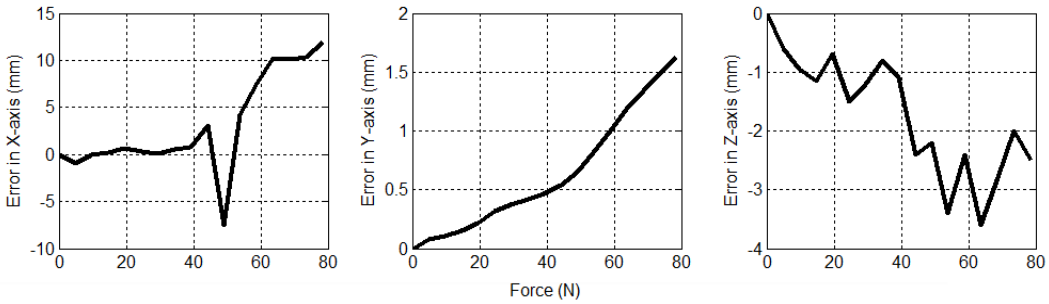

Fig. 11. Euclidean errors, along *X*, *Y* and *Z*-axis, between CCKA and Solidworks simulation

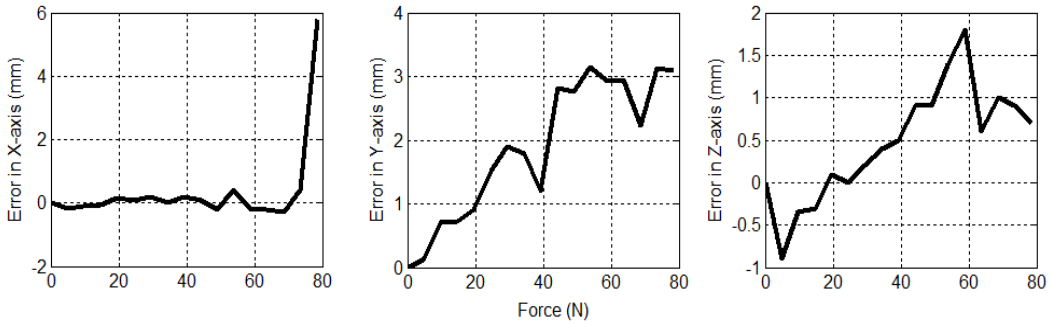

Fig. 12. Euclidean errors, along *X*, *Y* and *Z*-axis, between CCKA and experimental measurements

As a general conclusion of this analysis, since there are small errors between the obtained results; this enables to validate the application of CCKA for the considered class of continuum robots namely CDCR and therefore this

hypothesis may be adopted for research studies. But, it should be mentioned that when there are other applied forces such as external loading and gravity, the CCKA does not stand anymore [1, 3, 7] which has to be addressed in the future works.

5. Conclusion

In this paper, a forward kinematic model of a 2-DOFs cable-driven continuum robot was developed, under the constant curvature kinematic assumption, which was used to investigate this hypothesis. For this purpose, two software and experimental measurements were used. The Matlab software was used to plot the results of FKM outputs. Whereas nonlinear dynamic Solidworks simulation and experimental measurement were employed to check the FKM outputs (i.e. CCKA). The mean errors obtained between CCKA and Solidworks simulation, and CCKA and experimental measurements are respectively 0.77 % and 0.37 % of the robot length which validates the application of CCKA for the considered class of continuum robots namely cable-driven continuum robot.

REFERENCES

[1]. *D. Trivedi, C. D. Rahn, W. M. Kier, et al.*, "Soft robotics: biological inspiration, state of the art, and future research", Applied Bionics and Biomechanics, **vol. 5**, 2008, pp. 99–117.

[2]. *G. Robinson, J. B. C. Davies*, "Continuum robots – a state of the art," In Proceedings of IEEE international conference on robotics and automation, Detroit, Michigan, 1999, pp. 2849–2854.

[3]. *I. A. Gravagne and I. D. Walker*, "Kinematic transformations for remotely-actuated planar continuum robots," In Proceedings of IEEE International Conference on Robotics and Automation, San Francisco, CA, 2000, pp. 19–26.

[4]. *R. J. Webster, B. A. Jones*, "Design and kinematic modeling of constant curvature continuum robots: A review," International Journal of Robotics Research, **vol. 29**, no. 13, 2010, pp. 1661–1683.

[5]. *M. W. Hannan, I. D. Walker*, "Kinematics and the implementation of an elephant's trunk Manipulator and other continuum style robots," Journal of Robotic Systems, **vol. 20**, no. 2, 2003, pp. 45–63.

[6]. *Y. Bailly, Y. Amirat*, "Modeling and control of a hybrid continuum active catheter for aortic aneurysm treatment," In Proceedings of IEEE International Conference on Robotics and Automation, 2005, pp. 936–941.

[7]. *B. A. Jones, I. D. Walker*, "Kinematics for multisection continuum robots," IEEE Transactions on Robotics, **vol. 22**, no. 1, 2006, pp. 43–55.

[8]. *C. Escande, P. M. Pathak, R. Merzouki, et al.*, "Modeling of multisection bionic manipulator: Application to robotino XT," In Proceedings of IEEE international conference on robotics and biomimetics (ROBIO), Phuket, Thailand, 2011, pp. 92–97.

[9]. *B. He, Z. Wang, Q. Li, et al.*, "An analytic method for the kinematics and dynamics of a multiple-backbone continuum robot," International Journal of Advanced Robotic Systems, **vol. 10**, 2013, pp. 1–13.

[10]. *A. Amouri, C. Mahfoudi, A. Zaatri, et al.*, "A metaheuristic approach to solve inverse kinematics of continuum manipulators, " Journal of systems and Control Engineering, **vol. 231**, no. 5, 2017, pp. 380–394.

[11]. *A. Amouri, A. Zaatri, C. Mahfoudi*, "Dynamic modeling of a class of continuum manipulators in fixed orientation", Journal of Intelligent and Robotic Systems, **vol. 91**, no. 3–4, 2018, pp. 413–424.

[12]. *I. S. Godage, G. A. Medrano Cerda, D. T. Branson, et al.*, "Modal kinematics for multi-section continuum arms", Bioinspiration and Biomimetics, **vol. 10**, 2015, pp. 1–20.

[13]. *F. Qi, F. Ju, D. Bai and al*, "Motion modelling and error compensation of a cable-driven continuum robot for applications to minimally invasive surgery, " The international journal of medical robotics and computer assisted surgery, **vol. 14,** no. 6, 2018, pp. 1–11.

[14]. *L. Wu, R. Crawford, and J. Roberts*, "Dexterity analysis of three 6-DOF continuum robots combining concentric tube mechanisms and cable driven mechanisms, " IEEE Robotics and Automation Letters, **vol. 2**, no. 2, 2017, pp. 514–521.

[15]. *S. Mosqueda, Y. Moncada, C. Murrugarra et al.*, " Constant Curvature Kinematic Model Analysis and Experimental Validation for Tendon Driven Continuum Manipulators," In Proceedings of the 15th International Conference on Informatics in Control, Automation and Robotics, **vol. 2**, 2018, pp. 211–218

[16]. *M. Gouasmi, M. Ouali, B. Fernini and al.*, "Kinematic modeling and simulation of a 2R robot using Solidworks and verification by Matlab/Simulink," International Journal of Advanced Robotic System, **vol. 9**, no. 6, 2012, pp. 1–13.

[17]. *F. Cheraghpour, M. Vaezi, R. Eddin Shoori Jazeh, et al.*, "Dynamic modeling and kinematic simulation of Staubli TX40 robot using Matlab/Adams co-simulation," In Proceedings of IEEE International Conference on Mechatronics, Istanbul, 2011, pp. 386–391.

[18]. *A. Bourebbou, M. Hacini , M. Assas et al*., " Toolpath simulation of 3-axis parallel machine tool using geometrical model," UPB Scientific Bulletin, Series D: Mechanical Engineering, vol. 80, no. 4, 2018, pp. 15-26.

[19]. *A. Amouri, C. Mahfoudi, A. Zaatri et al.*, "Design, modeling and simulation of a cable-driven continuum robot using Matlab software and verification by real measurements," In Proceedings of the 3rd International Conference on Electromechanical Engineering (ICEE'2018). Skikda, Algeria, 21–22 November 2018.